

tance. The frame in the middle shows the structure outlined above, with both radiative cooling and thermal conduction at work in the hot gas. The top frame shows the same results, but now assuming that the shocked wind is able to instantaneously cool down to a temperature of 8,500 K, the same as the ambient gas. The shape of the bow shock is in this case much more irregular; this is due to the chaotic motions induced by Kelvin-Helmholtz instabilities when the gases coming from the ambient medium and from the stellar wind, having very different velocities along the bow shock, get in contact. Finally, the bottom frame is the same as the middle one, but now without allowing energy transport by thermal conduction. Also in

this case, the bow shock becomes unstable, with ripples and filaments appearing all along its inner surface. The sharper jump in density from the shocked wind to the bow shock is also apparent in this case. These simulations are described in detail by Comerón & Kaper (1997, in preparation).

In conclusion, we see that the observation of a wind bow shock around Vela X-1 provides support for Blaauw's scenario for the production of runaway stars. The wind bow shock itself provides an interesting laboratory to study the hydrodynamical processes involved in the collision of stellar wind particles moving at 1% of the speed of light with the interstellar medium that "approaches" the star with a supersonic velocity.

## References

- Blaauw, A. 1961, *Bull. Astr. Inst. Neth.* **15**, 265.  
 Blaauw, A. 1993, in *ASP Conf. Series*, Volume **35**, p. 207.  
 Gies, D.R. 1987, *ApJ Supp. Ser.* **64**, 545.  
 Gies, D.R., Bolton, C.T. 1986, *ApJ Supp. Ser.* **61**, 419.  
 Kaper, L., et al. 1997, *ApJ* **475**, L37.  
 Philp, C.J., et al. 1996, *AJ* **111**, 1220.  
 Poveda, A., et al. 1967, *Bol. Obs. Ton. y Tac.* **4**, 860.  
 Van Buren, D., McCray, R. 1988, *ApJ* **329**, L93.  
 Van Buren, D., et al. 1995, *AJ* **110**, 2914.  
 Van Rensbergen, W., et al. 1996, *A&A* **305**, 825.

L. Kaper  
 lkaper@eso.org

# Oph 2320.8–1721, a Young Brown Dwarf in the $\rho$ Ophiuchi Cluster: Views from the Ground and from Space

F. COMERÓN, ESO

P. CLAES, ESA, Villafranca del Castillo, Spain

G. RIEKE, Steward Observatory, Tucson, Arizona, USA

A variety of observational techniques have provided over the last few years the first reliable identifications of brown dwarfs and extrasolar planets, detected either by direct observations or by the gravitational effects on the stars they orbit. The list of the best brown-dwarf candidates known so far includes members of multiple systems, cluster members, and free-floating objects, as well as moderately young and more evolved objects. Likewise, the list of probable extrasolar planets, although still short, already includes objects covering a fairly large range of masses, distances to the central star, and eccentricities, thus suggesting the existence of several different scenarios for their formation and orbital evolution. The combination of new observational data and theoretical developments is leading to a vigorous activity in this field (Rebolo, 1997).

The observation of brown dwarfs in their earliest evolutionary stages is an important ingredient in our understanding of the formation and the characteristics of substellar objects. These objects sample a particular region of the temperature-surface gravity diagram, already abandoned by the more evolved objects discovered so far. They are still bright and hot, emitting most of their luminosity in the near-infrared. Their presence in clusters allows the study of coeval samples with well-constrained ages, and the determination of the mass func-

tion down to substellar masses. One of the best-studied very young, nearby clusters is the one near  $\rho$  Ophiuchi, usually referred to as "the  $\rho$  Ophiuchi cluster". Its proximity to the Sun (160 pc) and its age (a few million years) places its brown dwarfs well within the reach of arrays operating in the near-infrared, where the abundant dust in which the cluster members are still embedded is much more transparent than at visible wavelengths. The dust also helps by providing a natural screen against background sources unrelated to the cluster, whose density per unit area is already reduced by the relatively large distance of the cluster to the galactic equator.

In practice, the identification of a brown dwarf in an embedded cluster is complicated by several factors. Such an identification has to be done based on the luminosity, which allows an estimate of the mass by means of theoretical models (Burrows et al., 1993, D'Antona & Mazzitelli, 1994) provided that the age of the object is known. Unfortunately, the luminosity is difficult to assess, as the foreground dust absorbs most of the energy emitted at short wavelengths, including the near-infrared where the intrinsic spectral energy distribution of the object peaks. Also, a part of the luminosity of the object can be reprocessed by a circumstellar disk or envelope, which is a common feature in very young objects. On the other hand, the rapid decrease of

the luminosity of a very low mass object with time requires a precise knowledge of the age for a reliable mass estimate. However, this is not so demanding in the case of brown dwarfs, due to the temporary stability in the luminosity output by deuterium burning in the core, which can last for a time comparable to the duration of the embedded stage. These problems were considered by Comerón et al. (1993, 1996), who were able to derive mass functions down to  $\sim 0.04 M_{\odot}$  for both  $\rho$  Ophiuchi and NGC 2024 using mostly J, H and K band photometry. Nevertheless, the masses of individual objects in each of those aggregates was rather poorly constrained, due to the difficulty of reconstructing the intrinsic spectral energy distribution from the available JHK photometry alone.

The possible substellar character of one of the most promising brown-dwarf candidates identified in  $\rho$  Ophiuchi, Oph 2320.8–1721, was already pointed out by Rieke & Rieke (1990), who tentatively assigned to it a mass of  $0.06 M_{\odot}$ . This estimate was further reduced by Comerón et al. (1993), based on the need of assuming a moderate circumstellar infrared excess to fit the available photometry. A major step in supporting the brown-dwarf nature of Oph 2320.8–1721 came from its spectrum in the  $2 \mu\text{m}$  region presented by Williams et al. (1995), whose features clearly confirmed the low photospheric temperature

(below 3000 K) inferred from the fits to the broad-band photometry. Those authors set an upper limit of  $0.05 M_{\odot}$  on the mass of this object.

Oph 2320.8–1721 was included in a list of targets prepared by us for observations with the Infrared Space Observatory (ISO). The purpose of these observations was to extend the photometry of the best brown-dwarf candidates in  $\rho$  Ophiuchi into longer wavelengths, and to probe the region where their luminosities would be dominated by circumstellar emission in case that moderate amounts of circumstellar material were present. The observations were carried out in March 1996 with ISOCAM, the imaging camera on board of ISO, in wavelengths ranging from 3.6 to  $6 \mu\text{m}$ . We could also perform observations of Oph 2320.8–1721 with the NTT in the R and I bands in April 1997, and new observations in the JHK bands with IRAC2 at the ESO-MPI 2.2-m telescope, also in April 1997. The latter were intended to check for a suspected variability of the object suggested by Williams et al. (1995), which was not confirmed.

These observations sample the spectrum of Oph 2320.8–1721 from 0.7 to  $6 \mu\text{m}$ . This extended coverage enables us to disentangle in a reliable way the reddening of the spectral energy distributions of the embedded objects caused by foreground dust from that caused by the circumstellar material. As a consequence, we can now obtain a much more solid estimate of the luminosity of this object, and therefore also of its mass. Selected images taken with the telescopes mentioned above in different bands are presented in Figure 1, where Oph 2320.8–1721 appears near the centre of the frames. The magnitude of the object ranges from 24.41 in R to 10.1 at  $6 \mu\text{m}$  (ISOCAM filter LW4). In addition, the object was detected from the ground at  $10.6 \mu\text{m}$  (Rieke & Rieke, 1990), with an approximate magnitude of 8.7.

To derive the intrinsic spectral energy distribution of Oph 2320.8–1721, we have used new theoretical pre-main-sequence evolutionary tracks (Burrows et al., 1997, in preparation), which yield essentially the same best fitting parameters as the models of Burrows et al., 1993 for this particular object. The foreground extinction is assumed to follow the wavelength dependence described by Rieke & Lebofsky (1985); although important deviations from a universal law are known to exist in star-forming regions such as  $\rho$  Ophiuchi, they are unlikely to be important in the far-red and infrared wavelengths used here (Mathis, 1990). To model the circumstellar excess, we have used a power law form characterised by a single parameter,  $n$ , as defined by Adams et al. (1987). This approximation is found to reproduce to a good degree of accuracy the models of disks around low-mass stars and circumstellar envelopes around protostars

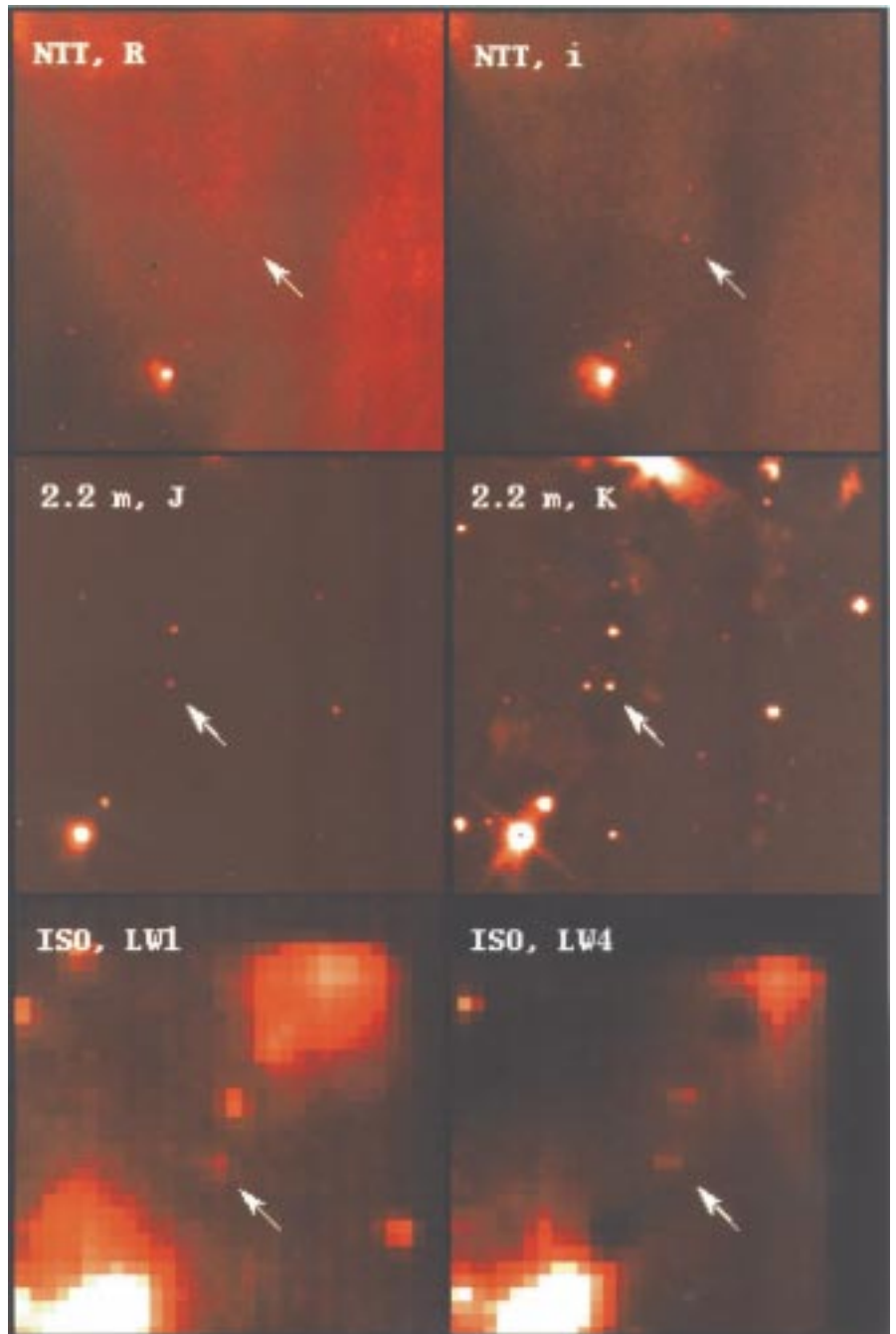


Figure 1: A mosaic of images of Oph 2320.8–1721 (pointed with an arrow) from 0.7 to  $6 \mu\text{m}$ . North is at the top and east to the left in the NTT and 2.2-m images; the ISO images are slightly rotated clockwise.

(Adams et al., 1987, Lada & Adams, 1992, Calvet et al., 1997). Finally, the photospheric fluxes at each band have been corrected for spectral features, mostly flux redistribution by wide molecular absorption bands, using approximate corrections to blackbody fluxes derived from the models of Allard & Hauschildt (1995).

Our best fit to the overall spectrum of Oph 2320.8–1721 is shown in Figure 2, and is represented by the solid line corresponding to a stellar photosphere plus a circumstellar disk reddened by foreground extinction. The dotted line represents the contribution to the luminosity from the stellar photosphere alone, reddened by the same amount of fore-

ground dust. Most of the difference between the two curves arises from light originally emitted by the central object at visible wavelengths which has been absorbed by the circumstellar disk, and then re-emitted in the mid-infrared. The rather poor fit of the measurements at R and I is probably due to the combined effect of the broad passband of those filters, the steep continuum spectral energy distribution of the object, and the complexity of the absorption features in that region. The best fit shown in Figure 2 is obtained for a luminosity of  $0.011 L_{\odot}$ , corresponding to a mass of  $0.04 M_{\odot}$ . This mass estimate does not change if the assumed age of the object is changed between 1.5 and 9 million

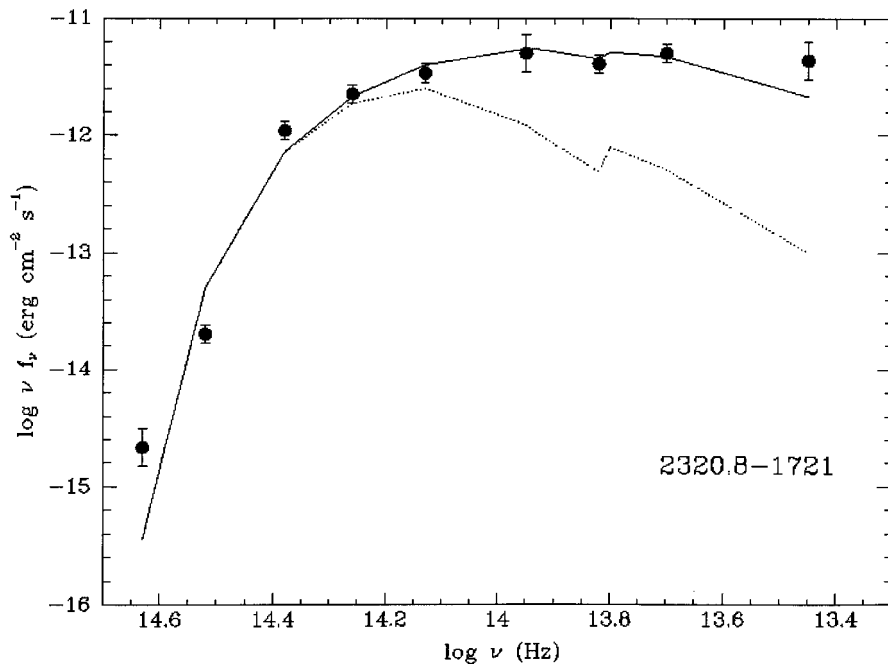


Figure 2: Best fit to the available photometry of Oph 2320.8–1721. The data points correspond from left to right to the following filters: R, I, J, H, K, L', ISOCAM LW1, ISOCAM LW4, and N. The solid line includes the contributions from the photosphere and the circumstellar excess, with the dotted line being the photospheric contribution alone. Both curves include a foreground reddening of  $A_V = 10$  mag.

years, and keeps below the stellar limit provided that the object is younger than 15 million years, which is more than the expected lifetime of an embedded cluster and several times the estimated age of the  $\rho$  Ophiuchi cluster. The circumstellar excess, characterised by a spectral index  $n = -1.6$  (where  $n = -3$  would correspond to a central source without circumstellar material and  $n > 0$  to a protostar totally embedded in its envelope) further supports the youth of Oph 2320.8–1721. The required foreground extinction to produce a good fit is  $A_V = 10$  mag, much less than the average extinction,  $A_V \sim 50$ , deduced from CO maps of the area, suggesting that Oph 2320.8–1721 is placed near the front edge of the cloud. The effective temperature of the object,  $T = 2650$  K, is

consistent with the spectral features discussed by Williams et al. (1995). On the other hand, due to the deuterium burning phase which Oph 2320.8–1721 is presumably undergoing, its age is practically unconstrained by our fits.

The long baseline in wavelength available with the new measurements, plus the insensitivity of the fit to the assumed age, make the above estimates much more robust than the ones presented in previous stages of this work. A significantly larger mass exceeding the stellar limit, implying a greater luminosity, would require a substantial increase in the amount of foreground extinction, which would be incompatible with the detection of the object in R. Moreover, this would decrease the required amount of circumstellar excess, making it inconsistent

with the rather flat shape of the  $\log(\nu f_\nu)$  curve at longer wavelengths. New, high signal-to-noise spectra of Oph 2320.8–1721 in the H and K regions obtainable in the near future with SOFI at the NTT would help to further constrain the surface temperature and gravity of this object, thus giving independent estimates of its temperature and luminosity. In the meantime, however, we can say that the identification of Oph 2320.8–1721 as a young brown dwarf is already supported by a very considerable amount of observational material.

**Acknowledgements:** We wish to thank Jason Spyromilio for making a part of his service observing time at the NTT available to us, as well as to the ESO staff providing support to the observations at the NTT and the 2.2-m telescope. Based on observations with ISO, an ESA project with instruments funded by ESA Member States (especially the PI countries: France, Germany, the Netherlands and the United Kingdom) with the participation of ISAS and NASA.

## References

- Adams, F.C., Lada, C.J., Shu, F.H., 1987, *ApJ*, **312**, 788.  
 Allard, F., Hauschildt, P.H., 1995, *ApJ*, **445**, 433.  
 Burrows, A., Hubbard, W.B., Saumon, D., Lunine, J.I., 1993, *ApJ*, **406**, 158.  
 Calvet, N., Hartmann, L., Strom, S.E., 1997, *ApJ*, **481**, 912.  
 Comerón, F., Rieke, G.H., Burrows, A., Rieke, M.J. 1993, *ApJ*, **416**, 185.  
 Comerón, F., Rieke, G.H., Rieke, M.J., 1996, *ApJ*, **473**, 294.  
 D'Antona, F., Mazzitelli, I., 1994, *ApJS*, **90**, 467.  
 Lada, C.J. Adams, F.C., 1992 *ApJ*, **393**, 278.  
 Mathis, J.S., 1990, *ARA&A*, **28**, 37.  
 Rebolo, R. (ed.), 1997, "Brown dwarfs and extrasolar planets", ASP Conf. Series, in press.  
 Rieke, G.H., Lebofsky, M.J., 1985, *ApJ*, **228**, 618.  
 Rieke, G.H., Rieke, M.J., 1990, *ApJ*, **362**, L21.  
 Williams, D.M., Comerón, F., Rieke, G.H., 1995, *ApJ*, **454**, 144.

F. Comerón  
 fcomeron@eso.org

# PMS Binaries in Southern Molecular Clouds Observed with ADONIS + COMIC

J.-L. MONIN and H. GEOFFRAY

Laboratoire d'Astrophysique – Observatoire de Grenoble, France

## 1. Introduction

The process of low-mass star formation is now well known for producing a large fraction of binary and multiple systems. This result is confirmed by many surveys (e.g. Reipurth & Zinnecker, 1993; Ghez et al., 1993; Leinert et al., 1993), showing that most, if not all, the

T Tauri stars (TTS) have companions. Therefore, the study of Pre-Main-Sequence (PMS) binary systems appears as a crucial key in understanding the process of star formation. However, due to the increasing number of multiple systems at small projected separations, the basic data do not exist for most of the individual members of these sys-

tems because of the limited angular resolution of the available instruments (cameras, spectrographs, and polarimeters), or the limited signal-to-noise ratio of the observations. For instance, some observations of PMS binaries have already been performed in Speckle at  $2.2 \mu\text{m}$  (Ghez et al., 1993), but this was mainly for a study of the binary-star fre-